Neurobiology of Disease

# Promoted Interaction of Nuclear Factor-κB with Demethylated Cystathionine-β-Synthetase Gene Contributes to Gastric Hypersensitivity in Diabetic Rats

**Hong-Hong Zhang,[1,2]* Ji Hu,[1]* You-Lang Zhou,[2,3]* Shufen Hu,[2] Yong-Meng Wang,[2] Wei Chen,[3] Ying Xiao,[1] Li-Yen Mae Huang,[4] Xinghong Jiang,[2] and Guang-Yin Xu[1,2]**

[1]Division of Endocrinology, the Second Affiliated Hospital, Soochow University, Suzhou 215000, P.R. China, [2]Institute of Neuroscience, Suzhou Key Laboratory of Pain Research and Therapy, Department of Neurobiology, Soochow University, Suzhou 215123, P.R. China, [3]Hand Surgery Research Center, Department of Hand Surgery, Affiliated Hospital of Nantong University, Nantong 226001, P.R. China, and [4]Department of Neuroscience and Cell Biology, University of Texas Medical Branch, Galveston, Texas 77555-1069

**Patients with long-standing diabetes frequently demonstrate gastric hypersensitivity with an unknown mechanism. The present study was designed to investigate roles for nuclear factor-κB (NF-κB) and the endogenous $H_2S$-producing enzyme cystathionine-β-synthetase (CBS) signaling pathways by examining *cbs* gene methylation status in adult rats with diabetes. Intraperitoneal injection of streptozotocin (STZ) produced gastric hypersensitivity in female rats in response to gastric balloon distention. Treatment with the CBS inhibitor aminooxyacetic acid significantly attenuated STZ-induced gastric hypersensitivity in a dose-dependent fashion. Aminooxyacetic acid treatment also reversed hyperexcitability of gastric-specific dorsal root ganglion (DRG) neurons labeled by the dye DiI in diabetic rats. Conversely, the $H_2S$ donor NaHS enhanced neuronal excitability of gastric DRG neurons. Expression of CBS and p65 were markedly enhanced in gastric DRGs in diabetic rats. Blockade of NF-κB signaling using pyrrolidine dithiocarbamate reversed the upregulation of CBS expression. Interestingly, STZ treatment led to a significant demethylation of CpG islands in the *cbs* gene promoter region, as determined by methylation-specific PCR and bisulfite sequencing. STZ treatment also remarkably downregulated the expression of DNA methyltransferase 3a and 3b. More importantly, STZ treatment significantly enhanced the ability of *cbs* to bind DNA at the p65 consensus site, as shown by chromatin immunoprecipitation assays. Our findings suggest that upregulation of *cbs* expression is attributed to *cbs* promoter DNA demethylation and p65 activation and that the enhanced interaction of the *cbs* gene and p65 contributes to gastric hypersensitivity in diabetes. This finding may guide the development and evaluation of new treatment modalities for patients with diabetic gastric hypersensitivity.**

## Introduction

Diabetes mellitus (DM) is a common disorder, with a worldwide prevalence of 6–7% (Watkins et al., 2000; Anitha et al., 2006). Diabetic gastrointestinal symptoms occur in as many as 75% of DM patients (Watkins et al., 2000; Bytzer et al., 2001). Abdominal pain or discomfort, one of the cardinal symptoms of gastrointestinal system in DM patients, has been a challenge for clinicians to treat effectively (Hoogerwerf et al., 1999; Vinik et al., 2003; Frøkjaer et al., 2011). The etiology of the gastrointestinal complications of DM is multifactorial. Several lines of evidence suggest that abdominal discomfort and pain are associated with altered function of primary afferent pathways (Srinivasan and Wiley, 2000; Chandrasekharan and Srinivasan, 2007) and the enteric nerves (Watkins et al., 2000; He et al., 2001).

Many previous studies have focused on the visceral hypersensitivity in the esophagus (Frøkjaer et al., 2007; Frøkjaer et al., 2009) and intestine (Beyak et al., 2009; Grabauskas et al., 2011) of rodents with experimental DM. Attention has not been well paid to diabetic visceral hypersensitivity in the stomach, an issue that is important for understanding gastrointestinal sensory dysfunction in peripheral sensitization because the stomach is affected in more than half of all diabetic patients (Liao et al., 2006). There is a growing body of evidence indicating that autonomic neuropathy is an important causal factor in diabetic gastropathy (Samsom et al., 1997; Watkins et al., 2000; Owyang, 2011). However, the mechanism underlying these changes in the primary sensory system in diabetic gastric hypersensitivity is not well defined.

Emerging evidence has indicated that activation of nuclear factor-κB (NF-κB) in dorsal root ganglia (DRG) neurons after peripheral inflammation or nerve injuries is related to generation

Received March 11, 2013; revised April 11, 2013; accepted April 16, 2013.

Author contributions: G.-Y.X. designed research; H.-H.Z., Y.-L.Z., S.H., Y.-M.W., and W.C. performed research; J.H., Y.-L.Z., S.H., Y.-M.W., and Y.X. analyzed data; H.-H.Z., J.H., L.-Y.M.H., X.J., and G.-Y.X. wrote the paper.

This work was supported by the National Natural Science Foundation of China (Grant #81070884 and Grant #81230024 to G.-Y.X. and Grant #31271258 to X.J.), the National Institutes of Health (Grant #NS30045 to L-Y.M.H.), and Jiangsu Province, China (Grant #SR21500111 to G.-Y.X.).

The authors declare no competing financial interests.

*H.-H.Z., J.H., and Y.-L.Z. contributed equally to this work.

Correspondence should be addressed to Dr. Guang-Yin Xu, Laboratory for Translational Pain Medicine, Department of Neurobiology, Institute of Neuroscience, Soochow University, 199 Ren-Ai Road, Suzhou 215123, P. R. China. E-mail: guangyinxu@suda.edu.cn.

DOI:10.1523/JNEUROSCI.1068-13.2013

 0270-6474/13/339028-11$15.00/0

of hyperalgesia or allodynia (Wang et al., 2011; Shi et al., 2013). We have recently reported that the endogenous $H_2S$-producing enzyme cystathionine-$\beta$-synthetase (CBS) played an important role in chronic visceral hypersensitivity (Xu et al., 2008; Xu et al., 2009; Li et al., 2012; Wang et al., 2012) and that peripheral inflammation led to *cbs* gene DNA demethylation (Qi et al., 2013), indicating a crucial role for CBS and an epigenetic mechanism in chronic pain (Zhang et al., 2011; Qi et al., 2013). However, roles for NF-$\kappa$B and CBS/$H_2S$ signaling in diabetic gastric hypersensitivity remain unknown. Therefore, we hypothesized that DM enhances *cbs* gene demethylation and promotes the interaction of activated NF-$\kappa$B with the *cbs* gene promoter, thus contributing to gastric hypersensitivity. To test this hypothesis, we examined how NF-$\kappa$B modulates *cbs* gene expression and determined the role of $H_2S$ in modulating excitability of stomach-projecting DRG neurons in an experimental rat model of diabetes. We demonstrated an upregulation of CBS and p65 expression, an increase in demethylation status of the *cbs* gene in the promoter region, and a potentiation of the ability of *cbs* to bind DNA at p65 consensus site in rats with diabetic visceral hypersensitivity in the stomach. Our findings illustrate an important role for NF-$\kappa$B and CBS/$H_2S$ signaling in diabetic gastric hypersensitivity.

## Materials and Methods

*Generation of streptozotocin-induced diabetic rats.* All experiments were approved by the institutional animal care and use committee at the Soochow University and the Association of Laboratory Animals in Jiangsu Province. Female Sprague Dawley rats weighing 150–180 g were housed four per cage in a 12 h/12 h light/dark cycle and temperature-controlled room (25 ± 1°C). Rats were allowed access to tap water and standard laboratory chow *ad libitum*.

Diabetes model was induced by a single intraperitoneal injection of streptozotocin (STZ; 65 mg/kg, Sigma), as described previously (Xu et al., 2011). STZ was freshly dissolved in citrate buffer (10 mmol/L, Na citrate, pH 4.3–4.4). The control (CON) group received citrate buffer only in an equivalent volume. One week later, diabetes was confirmed by measurements of blood glucose concentrations in samples obtained from the tail vein. Only rats with blood glucose concentration >15 mmol/L (270 mg/dL) were further used in the study.

*Implantation of gastric distension balloon and electrodes.* A total of 44 SD rats were used for electromyographic (EMG) recordings. Rats, fasted overnight, were deeply anesthetized with chloral hydrate (360 mg/kg body weight) and all surgical procedures were performed under sterile conditions. The procedure for the insertion of the gastric distension (GD) balloon was as described previously (Liu et al., 2011) with some modifications. Briefly, a 2.5-cm-long balloon (made from latex condoms) was attached to a catheter (PE-90). A 3- to 4-cm-long left lateral epigastric incision was made and the balloon was placed in the stomach through a small hole made at the tip of the fundus. When placed properly and not inflated, the pylorus was not obstructed and there was no blockage of gastric emptying. The hole was then securely tied to avoid leakage of gastric fluid into the peritoneum. The polyethylene tubing for air inflation of the gastric balloon was exteriorized at the back of the neck along with the EMG electrode leads. After balloon implantation, the abdominal cavity and skin incisions were closed.

To record EMG activities, sterilized, multistranded, Teflon-insulated, 40-gauge stainless steel wires (Cooner Wire) were implanted in the acromiotrapezius, a superficial neck muscle, using aseptic techniques and the incision was closed with a 4–0 silk suture. The electrode leads were externalized at the back of the head for easy access during experiments.

*EMG recordings.* One week after surgery, rats were given a single intraperitoneal injection of STZ (65 mg/kg, $n = 29$) or the same volume of solvent ($n = 15$). Two weeks later, seven rats from each group were tested weekly for EMG responses to graded gastric balloon distention (distention pressure, 60–120 mmHg). Response to GD was defined as an increase in EMG activity above baseline during the 20 s GD period. Data are reported as the area under curve (AUC) of the integrated EMG after baseline subtraction. We did not measure EMG responses at times beyond 6 weeks after balloon implantation because the latex balloon was weakened by prolonged exposure to low stomach pH. The rest of the STZ rats ($n = 22$) and CON rats ($n = 8$) were used to study the effect of the CBS inhibitor aminooxyacetic acid (AOAA) on behavior. Four weeks after STZ injection, 22 rats were divided into four groups and received an intraperitoneal injection of normal saline (NS; $n = 5$), AOAA 2.5 mg/kg ($n = 5$), AOAA 5 mg/kg ($n = 7$), or AOAA 10 mg/kg ($n = 5$). Age- and sex-matched CON rats received AOAA injection (5 mg/kg, i.p., $n = 8$). EMGs were recorded 30, 60, 90, and 120 min after AOAA treatment.

*Cell retrograde labeling.* The origin of the primary afferent innervation of the stomach was determined by retrograde tracing using DiI (Invitrogen). Experiments were performed on 12 female Sprague Dawley rats (150–160 g). Food, but not water, was withheld for 24 h before surgery. The animals were anesthetized with chloral hydrate (360 mg/kg). The stomach was exposed by midline abdominal incision, and DiI (25 mg in 0.5 ml methanol) was injected into the ventral (eight sites) and dorsal (eight sites) walls of the fundus, corpus, or pyloric antrum of the stomach with a Hamilton microsyringe. The volume of DiI injected at each site was 1 $\mu$l. To prevent leakage, the needle was left in place for 1 min after each injection. One week later, nine rats were given STZ and the other three rats received NS injection intraperitoneally. Four weeks later, bilateral thoracic T7–T10 DRGs from CON ($n = 3$) and STZ rats ($n = 3$) were dissected out for the excitability study using patch-clamp recordings. The other six STZ rats were divided into two groups ($n = 3$ for each group). Three weeks after STZ injection, these rats received either NS or AOAA intraperitoneal injection at 5 mg/kg once daily for seven consecutive days. The bilateral T7–T10 DRGs were dissected out for the study of changes in excitability of gastric projection neurons after AOAA treatment.

*Whole-cell patch-clamp recordings.* Changes in neuronal excitability were determined by whole-cell patch-clamp recording techniques as described previously (Xu et al., 2011). In brief, T7–T10 DRGs were dissected out and incubated in oxygenated dissection solution with enzymes (collagenase D, 1.5–1.8 mg/ml, and trypsin, 1.2 mg/ml; Sigma) for 1.5 h at 34.5°C. The dissection solution contained the following (in mM): 130 NaCl, 5 KCl, 2 $KH_2PO_4$, 1.5 $CaCl_2$, 6 $MgSO_4$, 10 glucose, and 10 HEPES, pH 7.2, osmolarity 305 mOsm. DRGs were then taken from the enzyme solution, washed, and transferred to the dissection solution containing DNase (0.5 mg/ml). A cell suspension was subsequently obtained by repeated triturationn through a series of flame-polished glass pipettes. Cells were then plated onto acid-cleaned glass coverslips. One coverslip containing adherent DRG cells was put into a small recording chamber (0.5 ml) attached to the stage of an inverted microscope (IX71; Olympus), which was fitted with both fluorescent and phase objectives. DiI-labeled neurons were identified by the bright red fluorescence in the cytoplasm. The currents were recorded in the external solution containing the following (in mM): 130 NaCl, 5 KCl, 2 $KH_2PO_4$, 2.5 $CaCl_2$, 1 $MgCl_2$, 10 HEPES, and 10 glucose, pH 7.2, adjusted with NaOH, osmolarity, 295–300 mOsm). Unless indicated, patch-clamp pipettes had a resistance of 3–5 M$\Omega$ when filled with the pipette solution containing the following (in mM): 140 potassium gluconate, 10 NaCl, 10 HEPES, 10 glucose, 5 BAPTA, and 1 $CaCl_2$, pH 7.25, adjusted with KOH, osmolarity, 295 mOsm). Resting potential (RPs) and action potentials (APs) were recorded. The voltage was clamped at −60 mV with a HEKA EPC10 patch-clamp amplifier. Capacitive transients were corrected using capacitive cancellation circuitry on the amplifier that yielded the whole-cell capacitance and access resistance. Up to 90% of the series resistance was compensated electronically. Considering the peak outward current amplitudes to be <10 nA, the estimated voltage errors from the uncompensated series resistance would be <10 mV. The leak currents at −60 mV were always <20 pA and were not corrected. The currents were filtered at 2–5 kHz and sampled at 50 or 100 $\mu$s/point. Whole-cell current and voltage were recorded with a HEKA EPC10 patch-clamp amplifier and data were acquired and stored on a computer for later analysis using FitMaster (HEKA). Patch-clamp recordings were performed at room temperature (~22°C).

*Western blot analysis.* The expressions of NF-$\kappa$B and CBS in T7–T10 DRGs from CON and STZ-treated rats were measured using Western

**Table 1. Oligonucleotides used in the study**

| Usage | Primers | Sequence (5′ to 3′) |
|---|---|---|
| RT-PCR | CBS-F | GAACCAGACGGAGCAAACAG |
| | CBS-R | GGCGAAGGAATCGTCATCA |
| | DNMT 3a-F | GAGGGAACTGAGACCCCAC |
| | DNMT 3a-R | CTGGAAGGTGAGTCTTGGCA |
| | DNMT 3b-F | CATAAGTCGAAGGTGCGTCGT |
| | DNMT 3b-R | ACTTTTGTTCTCGCGTCTCCT |
| | TGD-F | AGGTGTGTGTGGCAGATGGTT |
| | TGD-R | CCTACTGTGTTCTCAGGAGCCTAC |
| | MBD2-F | AAGAACCCTGCTGTTTGGCT |
| | MBD2-R | TTCTTTCGGACTTGTTGGACTC |
| | MBD4-F | AATATGGCAACGACTCCTACCG |
| | MBD4-R | GCTTCAGACAGGCGGCTTTA |
| | ACTIN-F | TCAGGTCATCACTATCGGCA |
| | ACTIN-R | GGCATAGAGGTCTTTACGGAT |
| MSP | *cbs*-M-F1 | AGTGTTTTTGAGCGTGGAGTC |
| | *cbs*-M-R1 | CAATTTACGAAACAACGATCTCC |
| | *cbs*-U-F1 | TTTAGTGTTTTTGAGTGTGGAGTT |
| | *cbs*-U-R1 | AAACAATTTACAAAACAACAATCTCC |
| | *cbs*-M-F2 | TGTGTTGGAACGTGATAGTTTTAC |
| | *cbs*-M-R2 | CCCAAACTTATCTTAACGAACGTA |
| | *cbs*-U-F2 | TTTGTGTTGGAATGTGATAGTTTTAT |
| | *cbs*-U-R2 | CCCAAACTTATCTTAACAAACATAAC |
| | *cbs*-M-F3 | TGTGTTGGAACGTGATAGTTTTAC |
| | *cbs*-M-R3 | TATCTTAACGAACGTAACCCAAA |
| | *cbs*-U-F3 | GTTTGTGTTGGAATGTGATAGTTTTAT |
| | *cbs*-U-R3 | TATCTTAACAAACATAACCCAAAACA |
| BSP | *cbs*-F | GGGAAGGTAGGTTTTTTATTTTGT |
| | *cbs*-R | AAACCACTCTTCCAATAAATTTTTC |
| ChIP | *cbs*/NF-κB-550-F | TCGCTGGGGTTCGGTAAC |
| | *cbs*/NF-κB-550-R | GGAAGTGGGCAACGGATG |
| | *cbs*/NF-κB-1050 –2F | GGGCGCGAGACTTAGGG |
| | *cbs*/NF-κB-1050 –2R | CCTCACGGAACAGAAAGCC |

BSP, Bisulfite sequencing PCR.

blot analysis. Rats were killed by an overdose of chloral hydrate. T7–T10 DRGs from both sides were quickly dissected out and put into oxygenated dissection solution. DRGs were lysed and centrifuged at 14,000 × *g* for 10 min. Protein samples were run on 12% Tris-HCl for 2 h at 80 V and then transferred to nitrocellulose membranes for 1.5 h at 200A. The membranes were blocked with StartBlock buffer for 2 h at room temperature. To measure the levels of NF-κB and CBS, anti-NF-κB (1:100) and anti-CBS (1:1000) were added, kept at 4°C overnight, and then washed in TBS with 0.1% Tween 20 for 1 h. The membranes were probed with corresponding horseradish peroxidase-conjugated secondary anti-rat antibodies at 1:2000 and 1:4000 dilution. Immunoreactive proteins were detected by enhanced chemiluminescence (ECL kit; GE Healthcare-Pharmacia Biotech). The densities of protein bands were analyzed using NIH Image software.

*RT PCR*. Total RNA was extracted from cells with TRIzol reagent (Invitrogen), and cDNA was synthesized from total RNA using an Omniscript RT kit 150 (QIAGEN) following the supplier's instructions. The sequences of the primers for CBS, DNA methyltransferase (DNMT) 3a and DNMT3b, thymine DNA glycosylase (TDG), methyl-binding domain protein 2 and 4 (MBD2 and MBD4), and actin (as an internal control) used in RT-PCR are shown in Table 1, and the cycle numbers used for amplification were 40, for CBS, DNMT3a and DNMT3b, TDG, MBD2, MBD4, and actin, respectively.

*Immunofluorescence study*. Five weeks after DiI injection, CON or STZ rats were perfused transcardially with 150 ml of PBS followed by 400 ml of ice-cold 4% paraformaldehyde in PBS. DRG T7–10 were removed and postfixed for 1 h in PFA and cryoprotected overnight in 20% sucrose in PBS. For triple labeling, 10-μm sections were simultaneously incubated with CBS (1:200; Abnova) and p65 (1:100; Abcam) antibodies and then incubated with Alexa Fluor 488 and Alexa Fluor 355. Negative control was performed by omitting the primary antibody. Sections were viewed with filter cubes appropriate for DiI (rhodamine filter), Alexa Fluor 488, and Alexa Fluor 355. Images were captured and analyzed using Metaview software. To ensure that a neuron was counted only once, serial sections were placed on consecutive slides with at least 50 μm between sections on the same slide.

*Methylation-specific PCR and sulfite sequencing*. The methylation status of the CpG island of all samples was initially screened at *cbs* gene promoter regions by methylation-specific PCR (MSP) as described previously (Herman et al., 1996; Kordi-Tamandani et al., 2010; Qi et al., 2013). When the CpG sites in the region analyzed by MSP were methylated, the methylated band would show up; conversely, the unmethylated band would be present when the sites were unmethylated. Occasionally, both bands could be present if the sites were partially methylated. The primers designed for *cbs* were as follows: MSP primers 1: methylated: forward 5′-AGTGTTTTTGAGCGTGGAGTC-3′, and reverse 5′-CAATTTACGAAACAACGATCTCC-3′; unmethylated: forward 5′-TTTAGTGTTTTTGAGTGTGGAGTT-3′, and reverse 5′-AAACAATTTACAAAACAACAATCTCC-3′. MSP primers 2: methylated: forward 5′-TGTGTTGGAACGTGATAGTTTTAC-3′, and reverse 5′-CCCAAACTTATCTTAACGAACGTA-3′; unmethylated: forward 5′-TTTGTGTTGGAATGTGATAGTTTTAT-3′, and reverse 5′-CCCAAACTTATCTTAACAAACATAAC-3′. MSP primers 3: methylated: forward 5′-TGTGTTGGAACGTGATAGTTTTAC-3′, and reverse 5′-TATCTTAACGAACGTAACCCAAA-3′; unmethylated: forward 5′-GTTTGTGTTGGAATGTGATAGTTTTAT-3′, and reverse 5′-TATCTTAACAAACATAACCCAAAACA-3′ (Table 1).

The methylation status was further validated by bisulfite sequencing (Frommer et al., 1992). Genomic DNA extracted from DRGs (T7–T10) was modified with bisulfite reagents following the manufacturer's instructions (Zymo Research). This modification resulted in a conversion of unmethylated cytosine to thymine, whereas the methylated cytosine remained unchanged. A total of 20 ng of bisulfite-modified DNA was subjected to PCR amplification and sequenced directly using the ABI 3700 automated sequencing system (Applied Biosystems). The following primers were designed to amplify CpG-rich regions within *cbs*: forward, 5′ GGGAAGGTAGGTTTTTTATTTTGT-3′, and reverse, 5′ AAACCACTCTTCCAATAAATTTTTC-3′ (Table 1).

*Chromatin immunoprecipitation assays*. The chromatin immunoprecipitation (ChIP) assay was done using the Millipore ChiP kit according to the manufacturer's instructions. Briefly, DRGs from STZ-induced diabetic rats and age- and sex-matched CON healthy rats were lysed for 10 min at 4°C and sonicated eight times for 15 s each. One-third of the lysate was used as the DNA input control. The remaining two-thirds were diluted 10-fold with ChIP dilution buffer supplied within the commercial kit, followed by incubation with an anti-p65 antibody or nonspecific control antibody (Santa Cruz Biotechnology) or mouse IgG (as a negative control) overnight at 4°C. Immunoprecipitated complexes were collected using protein G-agarose beads. The precipitates were extensively washed and then incubated in the elution buffer (1% SDS and 0.1 M $NaHCO_3$) at room temperature for 15 min. Cross-linking of protein-DNA complexes was reversed at 65°C for 4 h, followed by treatment with 10 mg/ml proteinase K for 1 h at 45°C. DNA was extracted with phenol/chloroform and precipitated with ethanol. Pellets were resuspended in Tris-EDTA buffer and subjected to PCR amplification using NF-κB consensus-site-specific primer 1 (forward: TCGCTGGGGTTCGGTAAC; reverse: GGAAGTGGGCAACGGATG) and specific primer 2 (forward: GGGCGCGAGACTTAGGG, reverse: CCTCACGGAACAGAAAGCC) in CBS promoter (Table 1). The resulting product was separated by 2% agarose gel electrophoresis.

*Data analysis*. No neuron with an RP more depolarized than −40 mV was included in the data analysis. All data are expressed as means ± SEM. Statistical analysis was conducted using OriginPro 8 (OriginLab), MATLAB (MathWorks), and SPSS statistics 17.0 software. Normality was checked for all data before analysis. Significance was determined using a 2-sample *t* test, Mann–Whitney test, Dunn's *post hoc* test after Friedman ANOVA, one-way ANOVA, two-way repeated-measures ANOVA followed by Tukey *post hoc* test, Kruskal–Wallis ANOVA followed by Tukey *post hoc* test, or $\chi^2$ test, as appropriate. $p < 0.05$ was considered statistically significant.

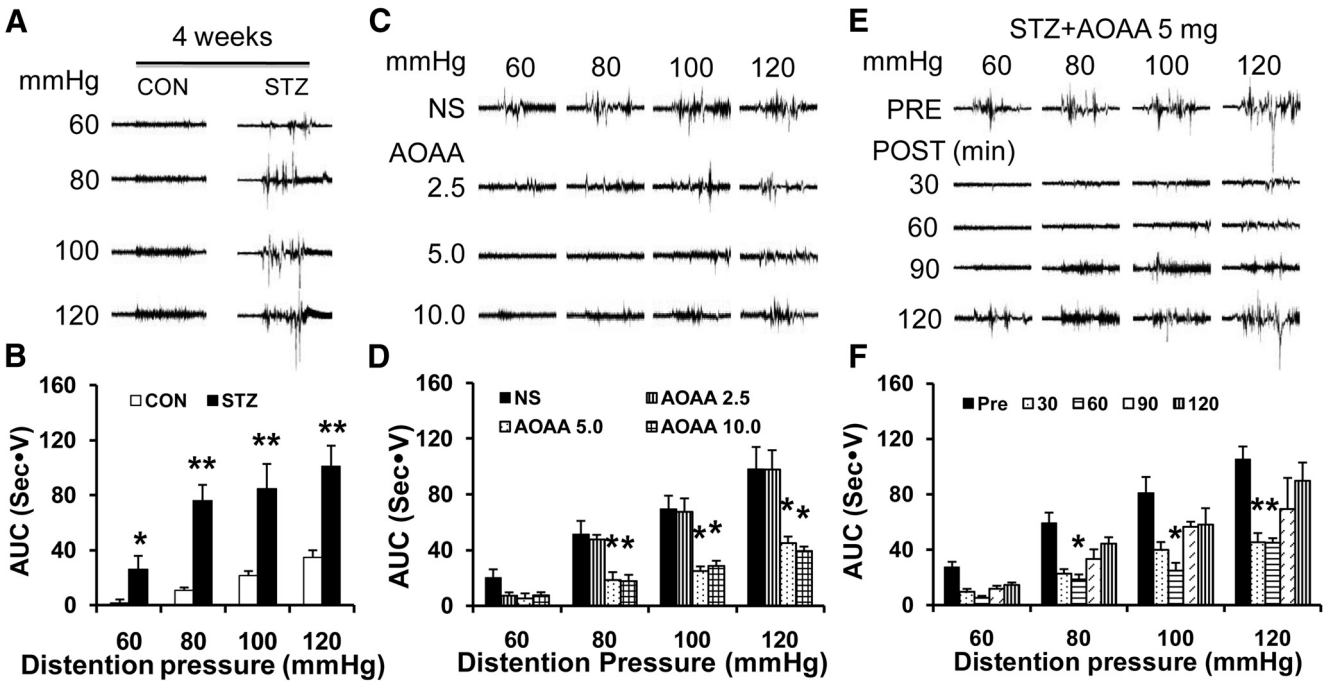


**Figure 1.** Inhibitory effect of the CBS inhibitor AOAA on gastric sensitivity. ***A***, Representative EMG recordings from CON and diabetic rats responding to graded GD at 60, 80, 100, and 120 mmHg 4 weeks after vehicle (CON) or STZ injection. ***B***, AUC of EMG recordings from the STZ group ($n = 7$) was significantly higher than CON ($n = 7$) at distention pressures of 60–120 mmHg ($^*p < 0.05$, $^{**}p < 0.01$, 2-sample *t* test and Mann–Whitney test after Friedman ANOVA). ***C***, Representative EMG recordings from diabetic rats in response to graded GD 60 min after a single injection of AOAA at doses of 2.5, 5, and 10 mg/kg body weight. ***D***, AOAA at doses of 5 mg/kg ($n = 7$) and 10 mg/kg ($n = 5$) dramatically suppressed EMG amplitude, whereas NS ($n = 5$) and AOAA at 2.5 mg/kg ($n = 5$) had no significant effect on EMG ($^*p < 0.05$ compared with NS at each pressure, Tukey *post hoc* test after one-way ANOVA). ***E***, Representative EMG recordings from diabetic rats in response to graded GD at different distention pressures between 60 and 120 mmHg after AOAA (5 mg/kg) treatment. ***F***, Bar graph showing that administration of AOAA resulted in a significant reduction on EMG responses of diabetic rats 60 min at 80, 100, and 120 mmHg distention pressures and 30 min at distention pressure of 120 mmHg ($n = 7$, $^*p < 0.05$ compared with before treatment, Dunn's *post hoc* test after Friedman ANOVA).

## Results

### STZ injection induces gastric hypersensitivity

STZ has been widely used to induce type 1 diabetes in rodents for the study of diabetic neuropathic pain (Grabauskas et al., 2011; Xu et al., 2011). In the present study, after a single intraperitoneal injection of STZ (65 mg/kg body weight), we monitored rat blood glucose level and body weight once every week for 5 weeks. In an agreement with our previously published data (Shi et al., 2013), the majority of rats (75.7%, $n = 117$) developed hyperglycemia after STZ injection. Blood glucose became elevated 1 week after STZ injection and stayed elevated for at least another 4 weeks (data not shown). Compared with CON rats, the growth rate of STZ rats was noticeably reduced (data not shown).

To record EMGs of the acromiotrapezius muscle responding to GD, implantation of gastric balloon and electrodes were made 1 week before injection of STZ ($n = 7$ rats) or CON ($n = 7$ rats). After recovery from surgery, GD-induced painful responses were recorded 2 weeks after STZ injection and recorded every week thereafter. Diabetic rats were more sensitive to graded gastric balloon distention as evident by the AUC. The results also showed that the significant effects were seen at distention pressures of 60, 80, 100, and 120 mmHg 4 weeks after STZ injection (Fig. 1*A*,*B*; $n = 7$ for each group, $^*p < 0.05$, $^{**}p < 0.01$, compared with CON, Mann–Whitney test after Friedman ANOVA). Gastric hypersensitivity in rats with diabetes was seen at 2 weeks at distention pressures of 100 and 120 mmHg and sustained through the next 3 weeks after STZ injection at all distention pressures compared with CON rats. The EMG amplitudes recorded 2, 3, and 5 weeks after injection of STZ or CON are not shown.

### CBS inhibitor AOAA treatment attenuates STZ-induced gastric hypersensitivity

$H_2S$ is increasingly thought to be an important molecular in the transmission and modulation of pain (Schemann and Grundy, 2009). To determine whether $H_2S$ is involved in development of gastric hypersensitivity in STZ rats, we observed the effect of an endogenous $H_2S$-producing enzyme, the CBS inhibitor AOAA, on EMG amplitude in response to GD (Fig. 1*C*,*D*). Four weeks after STZ treatment, a total of 22 diabetic rats with intragastric balloons were administrated AOAA in different doses (2.5, 5, and 10 mg/kg, i.p.). EMG recordings were recorded from diabetic rats in response to graded GD 30 min after AOAA treatment. NS and AOAA at the lowest dose (2.5 mg/kg) had no significant effect on EMG amplitude. However, AOAA at 5 and 10 mg/kg resulted in a dramatic reduction in EMG responses at 80–120 mmHg GD pressures (Fig. 1*C*,*D*; $n = 5$, 5, 7, and 5 for the NS group and the 2.5, 5, and 10 mg/kg AOAA groups, respectively, $^*p < 0.05$, compared with NS at each pressure, Tukey *post hoc* test after one-way ANOVA).

Because AOAA at the moderate dose of 5 mg/kg produced the maximal effect, we used this dose to determine the time course of AOAA effects. As shown in Figure 1*E*, *F*, the AOAA-induced analgesic effect lasted for ~60 min at 80, 100, and 120 mmHg distention pressures ($n = 7$, $^*p < 0.05$ compared with before treatment, Dunn's *post hoc* test after Friedman ANOVA). NS treatment did not affect the AUC of STZ rats. In addition, AOAA at 5 mg/kg did not produce a significant effect on AUC of EMG in age- and sex-matched healthy CON rats (data not shown).

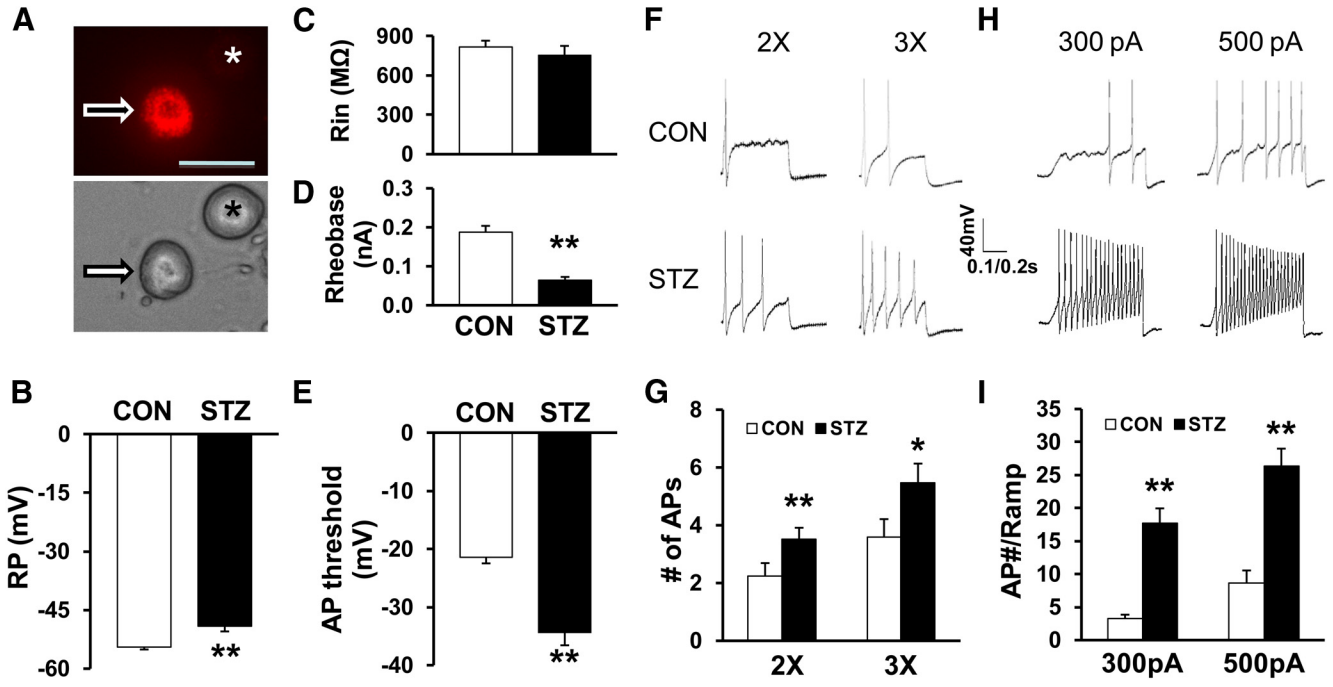


**Figure 2.** Enhanced excitability of gastric projection DRG neurons. ***A***, Top: Example of a DiI-labeled DRG neuron (arrow). Asterisk indicates the place where a neuron is not labeled by DiI. Bottom: Phase image of the same DRG neuron labeled by DiI is shown on the left (arrow) and the neuron not labeled by DiI is shown on the right (*). Scale bar, 50 $\mu$m. Patch-clamp recordings were performed on DiI-labeled colon neurons. A total of 20 DiI-labeled neurons form CON rats and 17 DiI-labeled neurons from STZ-treated rats were recorded under current-clamp conditions. ***B***, STZ injection significantly depolarized RPs of gastric projection DRG neurons (**$p < 0.01$ compared with CON, Mann–Whitney test). ***C***, STZ injection did not significantly alter $R_{in}$ compared with CON (STZ, $n = 17$, CON, $n = 20$, $p > 0.05$ compared with CON, Mann–Whitney test). ***D***, STZ injection markedly reduced rheobase (**$p < 0.01$ compared with CON, 2-sample $t$ test). ***E***, STZ injection remarkably hyperpolarized AP threshold (**$p < 0.01$ compared with CON, Mann–Whitney test). ***F***, ***G***, STZ injection also greatly increased numbers of APs evoked by 2× and 3× rheobase current stimulation (*$p < 0.05$, **$p < 0.01$ compared with CON, Mann–Whitney test). ***H***, Examples of APs by 300 and 500 pA ramp current injection from CON (top) and diabetic (bottom) rats. ***I***, Bar graph showed a significant increase in numbers of APs evoked by 300 pA and 500 pA ramp current stimulation in STZ-injected rats (**$p < 0.01$ compared with CON, 2-sample $t$ test).

### STZ injection enhances excitability of gastric projection DRG neurons

To determine whether primary sensory afferents are involved in the development of gastric hypersensitivity in STZ rats, we measured the excitability of gastric-specific DRG neurons from CON and STZ rats. Gastric-specific DRG neurons were labeled by the fluorescent dye DiI injected into the stomach wall. The small- and medium-sized DRG neurons (Fig. 2*A*) were used in this study because they are the primary sensory neurons responsible for pain sensation (Hunt and Mantyh, 2001; Xu and Huang, 2002). Under current-clamp conditions, a total of 37 cells were recorded. RPs were $-54.5 \pm 0.6$ mV ($n = 20$) and $-49.1 \pm 1.4$ mV ($n = 17$) for gastric-specific DRG neurons isolated from CON and STZ-injected female rats, respectively. Therefore, STZ injection significantly depolarized RP (Fig. 2*B*; **$p < 0.01$ compared with CON, Mann–Whitney test). The membrane input resistance ($R_{in}$) was $817.5 \pm 47.7$ MΩ ($n = 20$) and $753.5 \pm 71.7$ MΩ ($n = 17$) for gastric projection DRG neurons isolated from CON and STZ-injected rats, respectively. $R_{in}$ was not markedly altered after STZ injection when compared with CON (Fig. 2*C*). The rheobase measurements were $0.19 \pm 0.02$ nA ($n = 20$) and $0.06 \pm 0.01$ nA ($n = 17$) for CON and STZ-injected rats, respectively. STZ injection also markedly reduced rheobase (Fig. 2*D*; **$p < 0.01$, compared with CON, 2-sample $t$ test). The AP thresholds were $-21.4 \pm 1.1$ mV ($n = 20$) and $-34.4 \pm 2.2$ mV ($n = 17$) for CON and STZ-injected rats, respectively. STZ injection remarkably hyperpolarized the AP threshold (Fig. 2*E*; **$p < 0.01$ compared with CON, Mann–Whitney test). STZ injection also greatly increased the number of APs evoked by 2× and 3× rheobase current stimulation (Fig. 2*F*,*G*; *$p < 0.05$, **$p < 0.01$ compared with CON, Mann–Whitney test). The numbers of AP evoked by 2× rheobase current stimulation were $2.3 \pm 0.4$ ($n = 20$) and $3.5 \pm 0.4$ ($n = 17$) from CON and STZ-injected rats, respectively. The numbers of AP evoked by 3× rheobase current stimulation were $3.6 \pm 0.6$ ($n = 20$) and $5.5 \pm 0.7$ ($n = 17$) for CON and STZ-injected rats, respectively. STZ injection also resulted in a dramatic increase in the numbers of APs evoked by 300 and 500 pA ramp current stimulation (Fig. 2*H*,*I*; **$p < 0.01$ compared with CON, 2-sample $t$ test). The numbers of APs evoked by 300 pA ramp current stimulation were $3.2 \pm 0.6$ ($n = 18$) and $17.7 \pm 2.3$ ($n = 15$) for CON and STZ-injected female rats, respectively. The numbers of AP evoked by 500 pA ramp current stimulation were $8.7 \pm 1.9$ ($n = 18$) and $26.3 \pm 2.7$ ($n = 15$) for CON and STZ-injected female rats, respectively. STZ injection significantly enhanced the numbers of APs in response to ramp current stimulation.

### AOAA treatment reverses enhanced excitability

Because AOAA inhibited EMG responses in diabetic rats, we next investigated whether AOAA affects the excitability of gastric-specific DRG neurons of diabetic rats. Under current-clamp conditions, a total of 18 cells were recorded from 3 diabetic rats treated with AOAA 5 mg/kg (i.p.) once a day for 7 consecutive days. A total of 19 cells were recorded from 3 diabetic rats treated with NS at the same volume. RPs were $-52.8 \pm 2.1$ mV ($n = 18$) and $-48.2 \pm 1.0$ mV ($n = 19$) for gastric projection DRG neurons isolated from AOAA and NS-treated rats, respectively. Therefore, AOAA treatment significantly hyperpolarized RP (Fig. 3*A*; *$p < 0.05$ compared with NS, 2-sample $t$ test). $R_{in}$ was $835.8 \pm 106.4$ MΩ ($n = 18$) and $786.9 \pm 74.8$ MΩ ($n = 19$) for gastric projection DRG neurons isolated from AOAA and NS-

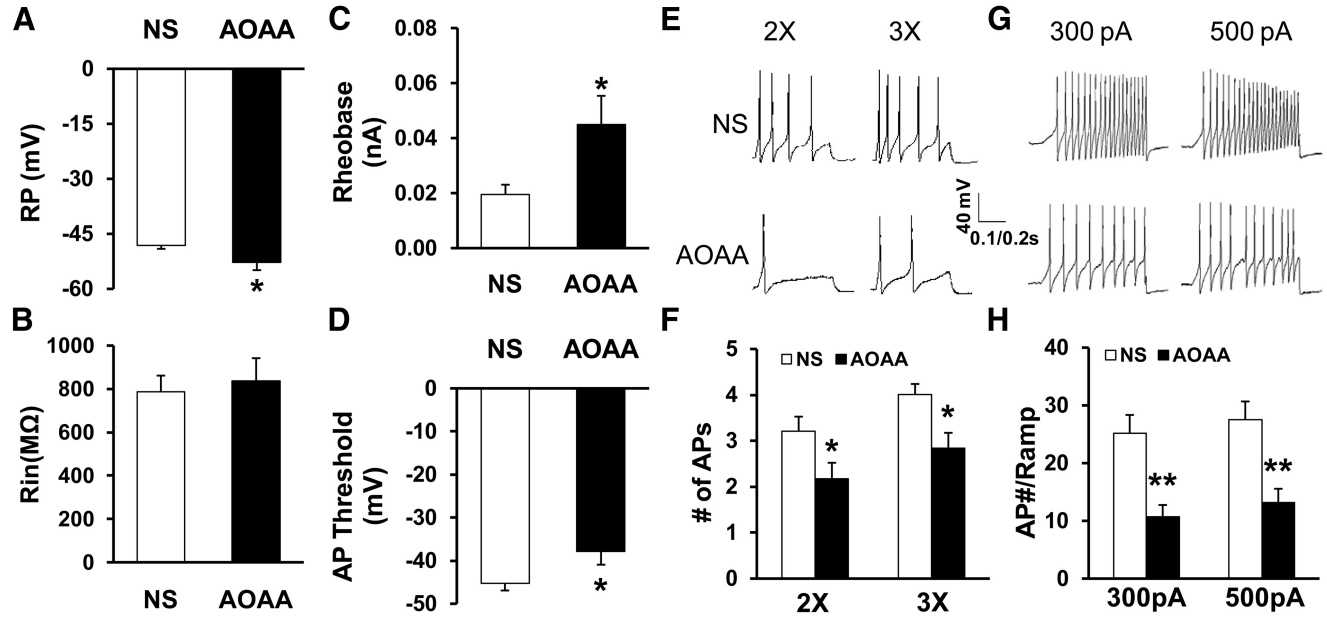


**Figure 3.** Reversal of neuronal hyperexcitability by the CBS inhibitor AOAA. ***A***, Administration of AOAA (i.p., 5 mg/kg once daily for consecutive 7 d) markedly hyperpolarized RP (AOAA, $n = 18$, NS, $n = 19$, $^*p < 0.05$ compared with NS, 2-sample $t$ test). ***B***, AOAA treatment did not significantly alter $R_{in}$ compared with CON (AOAA, $n = 18$, NS, $n = 19$, $p > 0.05$ compared with NS, Mann–Whitney test). ***C***, Administration of AOAA remarkably increased rheobase (AOAA, $n = 18$, NS, $n = 19$, $^*p < 0.05$ compared with NS, Mann–Whitney test). ***D***, AOAA treatment significantly increased AP threshold (AOAA, $n = 18$; NS, $n = 19$, $^*p < 0.05$ compared with NS, 2-sample $t$ test). ***E***, ***F***, AOAA treatment also greatly reduced numbers of AP evoked by 2× and 3× rheobase current stimulation (AOAA, $n = 18$, NS, $n = 19$, $^*p < 0.05$, Mann–Whitney test). ***G***, Examples of APs by 300 pA and 500 pA current injection from AOAA and NS-treated rats. ***H***, Bar graph showed a significant decrease in numbers of APs evoked by 300 and 500 pA ramp stimulation in AOAA-treated diabetic rats (AOAA, $n = 15$, NS, $n = 18$, $^{**}p < 0.01$ compared with NS, Mann–Whitney test).

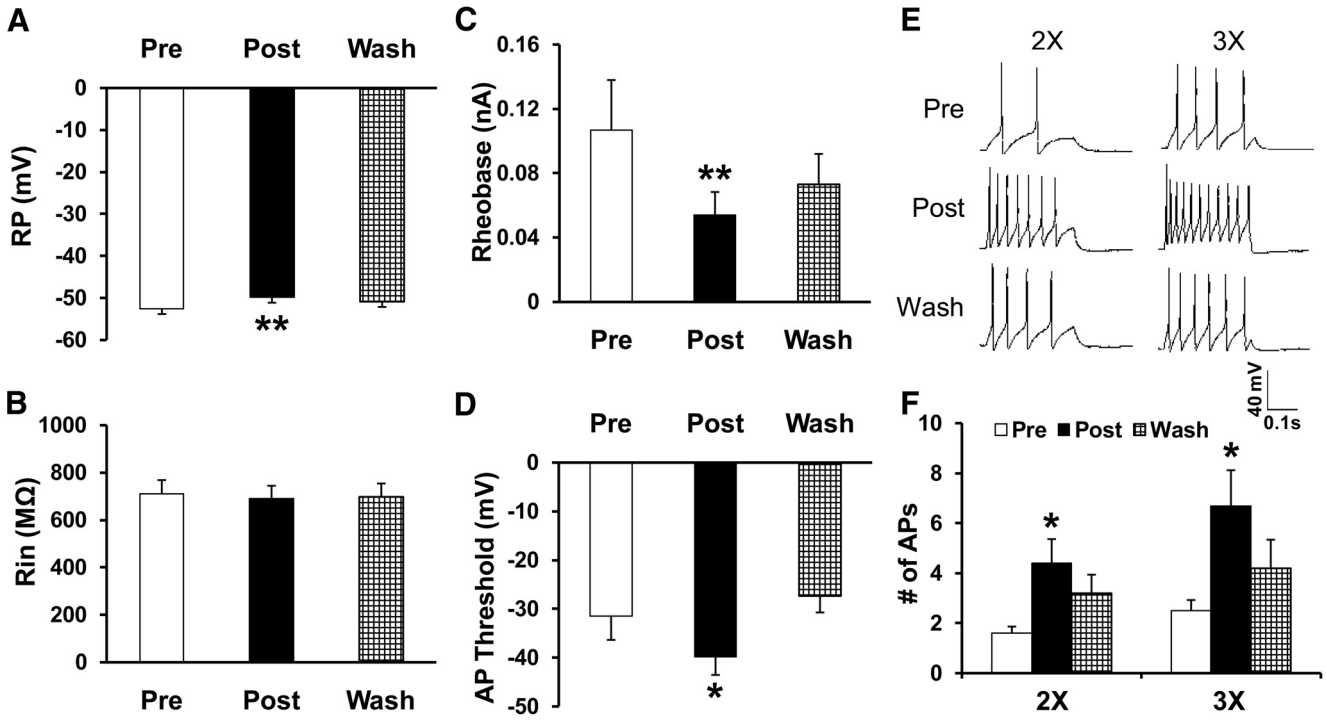


**Figure 4.** Increase in excitability by NaHS, a donor of $H_2S$, applied at 250 $\mu$M to gastric-specific DRG neurons from healthy female CON rats mimics the effect of CBS in producing $H_2S$. ***A***, Application of NaHS significantly depolarized RPs ($n = 10$, $^{**}p < 0.01$ compared with before treatment, one-way repeated-measures ANOVA). ***B***, Application of NaHS did not markedly alter $R_{in}$ ($n = 10$, $p > 0.05$ compared with before treatment, one-way repeated-measures ANOVA). ***C***, NaHS markedly reduced rheobase of DiI-labeled DRG neurons ($n = 10$, $^{**}p < 0.01$ compared with before treatment, one-way repeated-measures ANOVA). ***D***, NaHS application decreased AP threshold of DiI-labeled DRG neurons ($n = 10$, $^*p < 0.05$ compared with before treatment, one-way repeated-measures ANOVA). ***E***, ***F***, NaHS also greatly increased numbers of AP evoked by 2× and 3× rheobase current stimulation ($n = 10$, $^*p < 0.05$ compared with before treatment, Friedman ANOVA followed by Dunn's *post hoc* test). Note that all of these effects are washouts.

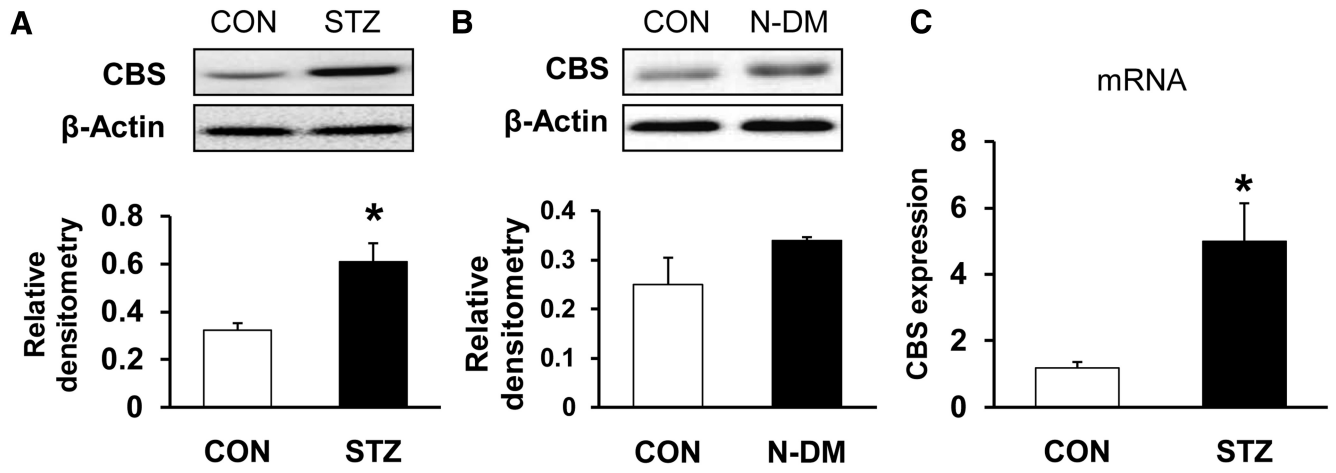


**Figure 5.** Upregulation of CBS expression. ***A***, CBS protein expression was greatly enhanced in diabetic rats compared with age- and sex-matched CON rats (CON, $n = 3$; STZ, $n = 4$, $^*p < 0.05$ compared with CON, 2-sample *t* test). ***B***, CBS protein expression was not altered in N-DM rats compared with age- and sex-matched CON rats (CON, $n = 3$; N-DM, $n = 3$, $p > 0.05$ compared with CON, 2-sample *t* test). ***C***, RT-PCR assays demonstrated a significant upregulation of CBS mRNA expression in T7–T10 DRGs in diabetic rats (CON, $n = 6$; STZ, $n = 4$, $^*p < 0.05$ compared with CON, 2-sample *t* test).

treated rats, respectively. $R_{in}$ was not markedly altered after STZ injection compared with CON (Fig. 3*B*). The rheobase measurements were 0.02 ± 0.0 nA ($n$ = 19) and 0.05 ± 0.01 nA ($n$ = 18) for the NS- and AOAA-treated groups, respectively. Administration of AOAA markedly increased rheobase (Fig. 3*C*; AOAA, $n$ = 18, NS, $n$ = 19, $^*p < 0.05$ compared with NS, Mann–Whitney test). AOAA treatment also increased the AP threshold (Fig. 3*D*; AOAA, −37.91 ± 3.05 mV, $n$ = 18; NS, −45.26 ± 1.69 mV, $n$ = 19, $^*p < 0.05$ compared with NS, 2-sample *t* test). In addition, AOAA treatment greatly reduced the number of APs evoked by 2× and 3× rheobase current stimulation (Fig. 3*E*,*F*; $^*p < 0.05$, Mann–Whitney test). The numbers of APs evoked by 2× rheobase current stimulation were 3.2 ± 0.3 ($n$ = 19) and 2.2 ± 0.2 ($n$ = 18) for the NS- and AOAA-treated groups, respectively. The numbers of APs evoked by 3× rheobase current stimulation were 4.0 ± 0.4 ($n$ = 19) and 2.8 ± 0.3 ($n$ = 18) for the NS- and AOAA-treated groups, respectively. The numbers of APs evoked by 300 pA ramp current stimulation were 25.2 ± 3.1 ($n$ = 18) and 10.7 ± 2.1 ($n$ = 15) for the NS- and AOAA-treated groups, respectively. The numbers of APs evoked by 500 pA ramp current stimulation were 27.5 ± 3.1 ($n$ = 18) and 13.1 ± 2.4 ($n$ = 15) for the NS- and AOAA-treated groups, respectively. AOAA treatment remarkably reduced the numbers of APs evoked by 300 pA and 500 pA ramp current stimulation (Fig. 3*G*,*H*; $^{**}p < 0.01$ compared with NS, Mann–Whitney test).

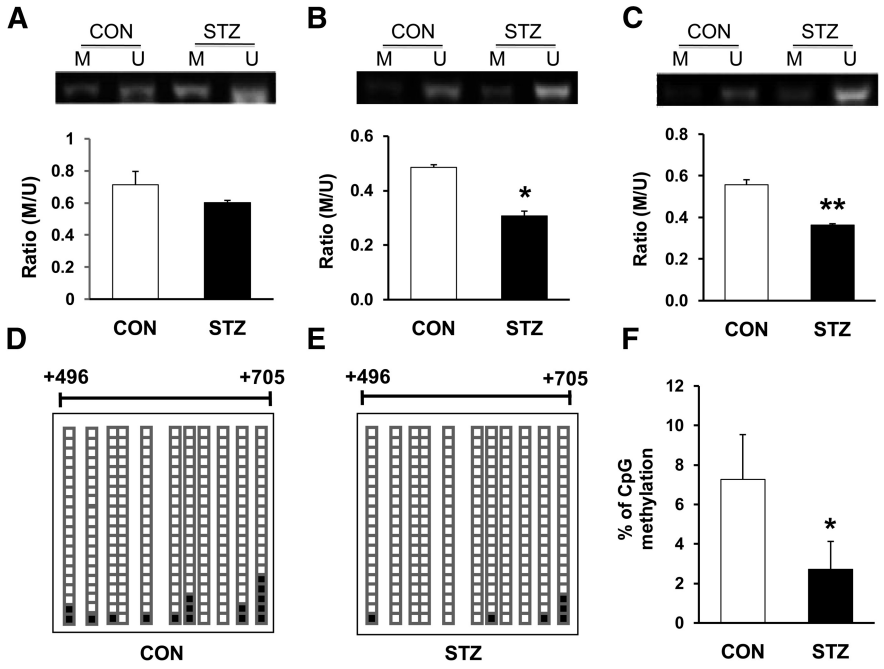


**Figure 6.** Demethylation of DNA in the *cbs* gene promoter. ***A–C***, Methylation status of the CpG island in the *cbs* gene promoter region was examined by MSP on T7–T10 DRGs from STZ-injected diabetic rats and age- and sex-matched CON rats. M indicates reactions using primer set specific for methylated CpG sites; U, reactions using primer set specific for unmethylated CpG sites. STZ injection significantly reduced the ratio of M/U for primer 2 (***B***) and 3 (***C***), but not for primer 1 (***A***, STZ, $n = 5$, CON, $n = 3$, $^*p < 0.05$, $^{**}p < 0.01$ compared with CON, 2-sample *t* test). ***D–F***, STZ injection produced significant demethylation of *cbs* gene in T7–T10 DRGs using bisulfite sequencing of the promoter region containing 11 CpG sites. Each square indicates the clones from CON rats (***D***) and STZ-injected rats (***E***). Twenty clones were subjected to bisulfite sequencing. The methylated clones for individual CpG sites (indicated in ***D*** and ***E***) are labeled in black. $^*p < 0.05$ compared with CON, $\chi^2$ test.

### NaHS treatment increases excitability of gastric projection DRG neurons

Since $H_2S$ is generated by CBS, we next investigated the role of $H_2S$ in neuronal excitability. NaHS, a donor for $H_2S$, was applied *in vitro* to gastric-specific DRG neurons. The addition of NaHS mimics the production of CBS for $H_2S$. Application of NaHS significantly depolarized RPs (Fig. 4*A*), but did not significantly alter $R_{in}$ (Fig. 4*B*). The RP before NaHS incubation (Pre) was −52.5 ± 1.34 mV ($n$ = 10). After NaHS application (Post) for 3 min, RP was −49.8 ± 1.34 mV ($n$ = 10, $^{**}p < 0.01$ compared with before treatment, one-way repeated-measures ANOVA). Application of NaHS also led to a marked reduction in rheobase (Fig. 4*C*). The rheobase before NaHS incubation was 0.11 ± 0.03 nA ($n$ = 10). After NaHS application for 3 min, rheobase was 0.05 ± 0.01 nA

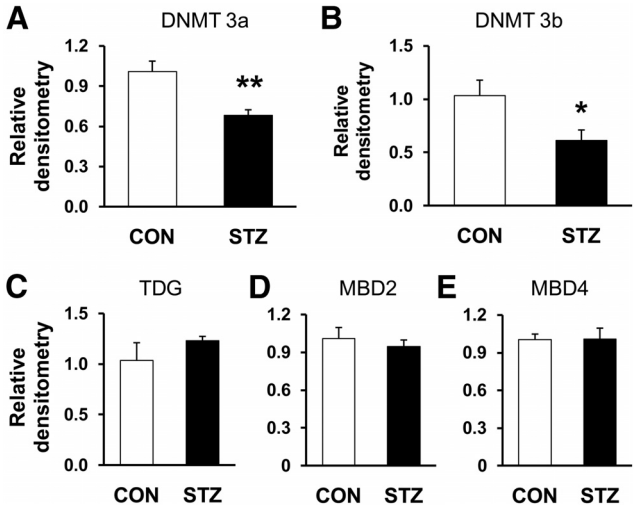


**Figure 7.** ***A***, ***B***, Suppression of DNMT3a and DNMT3b expression. RT-PCR assays demonstrated a significant downregulation of DNMT3a (***A***) and DNMT3b (***B***) mRNA expression in T7–T10 DRGs in diabetic rats compared with age- and sex-matched CON rats (CON, $n = 4$, STZ, $n = 8$, $^{*}p < 0.05$, $^{**}p < 0.01$, 2-sample *t* test). ***C***–***E***, STZ injection did not alter expression of TDG (***C***), MBD2 (***D***), and MBD4 (***E***) in T7–T10 DRGs compared with age- and sex-matched CON rats (CON, $n = 4$, STZ, $n = 8$, $p > 0.05$, 2-sample *t* test).

($n = 10$, $^{**}p < 0.01$ compared with before treatment, one-way repeated-measures ANOVA). The RP and rheobase returned to baseline after washing (Wash). Incubation of NaHS also decreased the AP threshold (Fig. 4*D*; before treatment, $-31.54 \pm 4.81$ mV; after treatment, $-39.79 \pm 3.75$ mV; after washing, $-27.36 \pm 3.38$ mV, $n = 10$, $^{*}p < 0.05$ compared with before, one-way repeated measure ANOVA). In addition, NaHS significantly increased the number of APs evoked by 2× and 3× rheobase current stimulation (Fig. 4*E*,*F*; 2×: before treatment, $1.60 \pm 0.27$; after treatment, $4.40 \pm 0.97$; after washing, $3.2 \pm 0.74$. 3×: before treatment, $2.50 \pm 0.43$; after treatment, $6.70 \pm 1.42$; after washing, $4.20 \pm 1.43$; $n = 10$, $^{*}p < 0.05$ compared with before treatment, Friedman ANOVA followed by Dunn's *post hoc* test).

### STZ injection upregulates CBS expression

To determine whether expression of CBS increased in T7–T10 DRGs after STZ injection, Western blot assays were performed. Proteins were isolated from both sides of T7–T10 DRGs of CON and STZ rats. After separating by electrophoresis under denaturing conditions, proteins were transferred to polyvinylidenedifluoride membranes and probed with anti-CBS antibody, which labeled a 62 kDa molecular weight protein (Fig. 5*A*). After STZ injection, the level of expression of CBS was increased significantly (Fig. 5*A*; CON, $n = 3$; STZ, $n = 4$, $^{*}p < 0.05$ compared with CON, 2-sample *t* test). To determine whether STZ itself upregulated CBS expression, proteins from T7–T10 DRGs from STZ-injected rats without hyperglycemia (blood glucose level < 15 mmol/L) were analyzed. As shown in Figure 5*B*, relative densitometry of CBS was $0.25 \pm 0.05$ and $0.34 \pm 0.01$, respectively, for CON rats and STZ-injected rats without hyperglycemia (N-DM). CBS expression in STZ-injected rats without hyperglycemia did not differ from CON rats ($p > 0.05$). CBS expression at the mRNA level was also measured. CBS mRNA was remarkably enhanced after STZ injection with hyperglycemia (Fig. 5*C*; CON, $n = 6$; STZ, $n = 4$, $^{*}p < 0.05$ compared with CON, 2-sample *t* test). Therefore, CBS expression was upregulated at both the transcriptional and protein levels after STZ-induced diabetes.

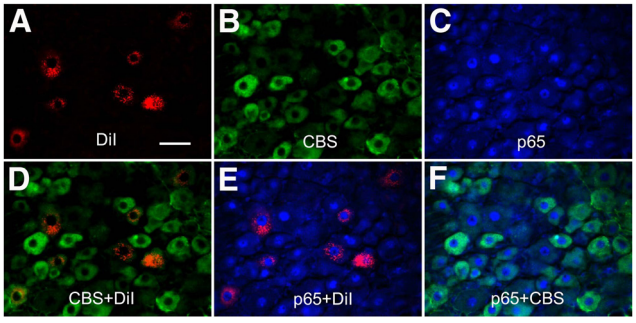


**Figure 8.** Coexpression of CBS with p65 in gastric projection DRG neurons. ***A***, Stomach T9 DRG cells were labeled with DiI (red) injected into the stomach wall. ***B***, CBS-positive cells are shown in green. ***C***, p65-positive cells are shown in blue. ***D***, Merge of double labeling of DiI and CBS. ***E***, Merge of p65-positive staining and DiI labeling. ***F***, Merge of p65-positive staining and CBS labeling. Scale bar, 50 $\mu$m.

### STZ injection enhances DNA demethylation of the *cbs* promoter by downregulation of DNMTs

Evidence suggests that DNA methylation suppresses gene expression (Turek-Plewa and Jagodziński, 2005). Therefore, we examined DNA methylation status at the promoter region of the *cbs* gene with an MSP assay. The genomic structure of the rat *cbs* gene, along with the fragment F210bp in the promoter region, were described previously (Qi et al., 2013). There are two CpG islands in the *cbs* gene. Because CpG island 2 (CpG2) contains more transcriptional factor binding sites (i.e., NF-κB; TFSEARCH program, version 1.3, available at: http://www.cbrc.jp/research/db/TFSEARCHJ.html), we focused on the methylation status of CpG2 in this study. We found that all samples yielded methylated and unmethylated bands from both CON and STZ-injected rats (Fig. 6*A*–*C*). Although the ratio of methylated to unmethylated CpG sites for MSP primers 1 (approximately +325/+425, Fig. 6*A*; STZ, $n = 5$, CON, $n = 3$, $p > 0.05$ compared with CON, 2-sample *t* test) was not significantly altered, STZ injection markedly reduced the methylated to unmethylated ratios for MSP primers 2 (approximately +657/+767, Fig. 6*B*; STZ, $n = 5$, CON, $n = 3$, $^{*}p < 0.05$ compared with CON, 2-sample *t* test) and for MSP primers 3 (approximately +657/+759, Fig. 6*C*; STZ, $n = 5$, CON, $n = 3$, $^{**}p < 0.01$ compared with CON, 2-sample *t* test), suggesting that there is significant demethylation within CpG2 of the *cbs* promoter region under STZ-induced gastric hypersensitivity conditions.

To further confirm methylation status of CpG sites within the *cbs* promoter area, DNA sequencing was performed on PCR products of the F210bp (approximately +496/+705) fragment obtained after treatment of genomic DNA samples with sodium bisulfite. As described previously (Qi et al., 2013), F210bp contains 11 CpG sites. All DRG samples from CON (Fig. 6*D*) and STZ-injected (Fig. 6*E*) rats were successfully sequenced. The percentage of methylation of the CpG sites within F210bp was significantly reduced in T7–T10 DRGs 4 weeks after STZ injection compared with age- and sex-matched CON rats (Fig. 6*F*; $n = 5$ for each group, $^{*}p < 0.05$ compared with CON, $\chi^2$ test), which is consistent with the results of the MSP assay.

We next investigated whether DNMTs are involved in methylation of the *cbs* gene. As shown in Figure 7*A*, *B*, STZ injection significantly reduced the expression of DNMT3a (Fig. 7*A*; CON, $n = 4$, STZ, $n = 8$, $^{**}p < 0.01$, 2-sample *t* test) and DNMT3b (Fig. 7*B*; CON, $n = 4$, STZ, $n = 8$, $^{*}p < 0.05$, 2-sample *t* test). We also examined the expression of TDG and MBD2 and MBD4 of T7–T10 DRGs in diabetic rats 4 weeks after STZ injection. However, the expression of TDG (Fig. 7*C*; CON, $n = 4$, STZ, $n = 8$, $p >$

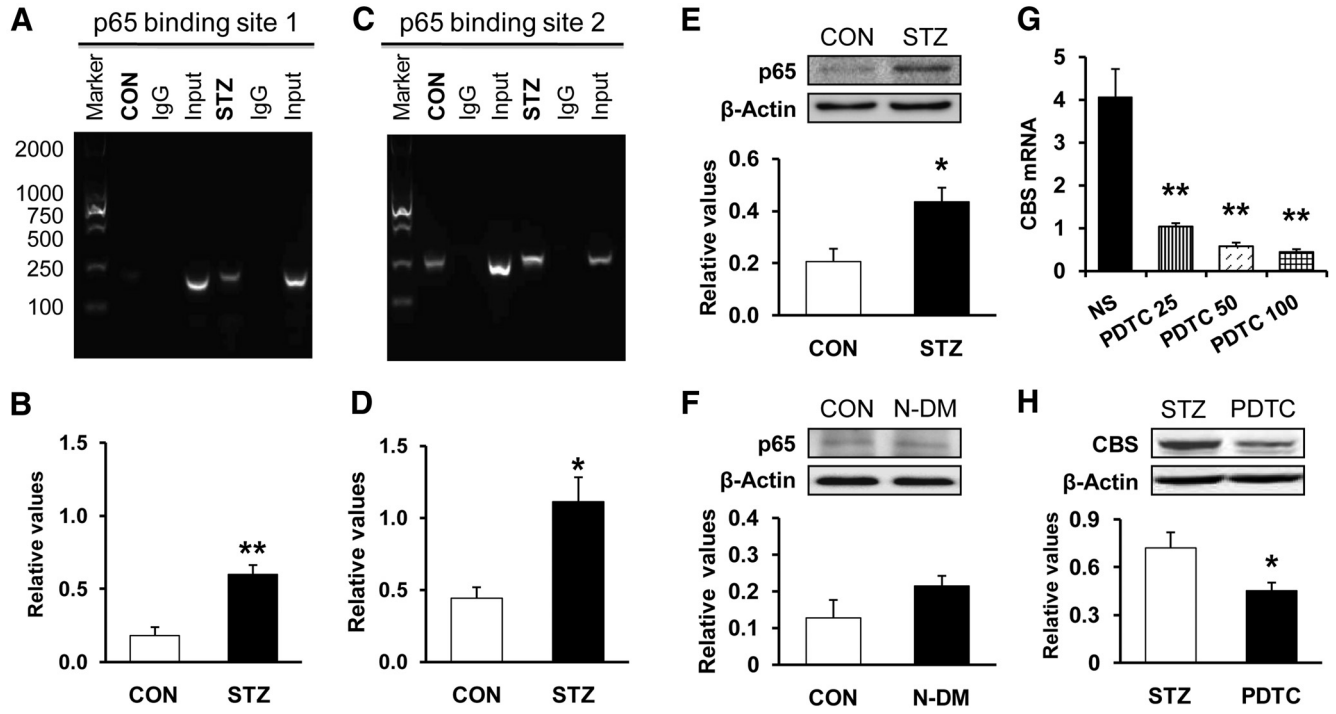


**Figure 9.** Potentiated interaction between NF-κB and *cbs* promoter regions. The specific anti-p65 antibody or CON normal mouse IgG was used for immunoprecipitation. ***A***, ***B***, Products of PCR amplifications for P1 (192 bp) and P2 (258 bp) from the proximal region of the *cbs* promoter. ChIP assays indicated a significant increase in binding activity of p65 with the first binding site of promoter of *cbs* gene in diabetic rats ($n = 3$ sample, 2 rats for each sample) compared with age- and sex-matched CON rats ($n = 3$ sample, 2 rats for each sample, $^{**}p < 0.01$ compared with CON, 2-sample *t* test). ***C***, ***D***, ChIP assays indicated a significant increase in binding activity of p65 with the second binding site of promoter of *cbs* gene in diabetic rats ($n = 3$ sample, 2 rats for each sample) compared with age- and sex-matched CON rats ($n = 3$, each for 2 rats, $^{*}p < 0.05$ compared with CON, 2-sample *t* test). ***E***, STZ injection significantly enhanced the expression of p65 in T7–T10 DRGs (CON, $n = 5$, STZ, $n = 4$, $^{*}p < 0.05$ compared with CON, 2-sample *t* test). ***F***, STZ injection did not significantly alter expression of p65 in T7–T10 DRGs in N-DM rats ($n = 4$) compared with CON ($n = 4$) ($p > 0.05$, 2-sample *t* test). ***G***, Administration of PDTC at different doses (once daily for consecutive 7 d) dramatically reduced the expression of CBS mRNA (STZ + NS, $n = 4$; $n = 3$ for other each group, $^{**}p < 0.01$ compared with STZ + NS group; Tukey *post hoc* test after one-way ANOVA). ***H***, Administration of PDTC (50 mg/kg once daily for consecutive 7 d) dramatically reduced CBS expression at the protein level (STZ + NS, $n = 4$; STZ + PDTC, $n = 5$, $^{*}p < 0.05$ compared with NS group, 2-sample *t* test).

0.05, 2-sample *t* test), MBD2 (Fig. 7*D*; CON, $n = 4$, STZ, $n = 8$, $p > 0.05$, 2-sample *t* test) and MBD4 (Fig. 7*E*; CON, $n = 4$, STZ, $n = 8$, $p > 0.05$, 2-sample *t* test) was not altered remarkably.

### STZ injection potentiates interaction of NF-κB with the *cbs* gene promoter

The molecular pathways involved in the regulation of CBS expression occur largely at a transcriptional level and appear to require NF-κB activation (Shi et al., 2013). Based on this evidence, and given the inhibitory effect of PDTC on CBS upregulation (Li et al., 2012), the potentiation of *cbs* gene demethylation, concomitantly with the upregulation of p65 at the same time point, prompted us to further explore the mechanism of CBS upregulation after STZ injection. We first investigated whether CBS was coexpressed in p65-positive gastric projection DRG neurons in healthy CON rats. Triple-labeling techniques were used in this experiment. Gastric projection DRG neurons were retrogradely labeled by DiI, as described above. DRG sections containing DiI-labeled neurons were stained with CBS and p65 antibodies. Approximately 95% of gastric projection DRG neurons that were immunoreactive for CBS were also positive for p65 (Fig. 8). Similarly, all gastric projection DRG neurons that were immunoreactive for p65 also were positive for CBS (Fig. 8).

The results of the ChIP assay revealed that nuclear extracts contain a protein complex that binds to p65 oligonucleotides from both CON and STZ rats. Although there was modest binding in extracts isolated from age- and sex-matched CON rats (Fig. 9*A*,*B*, lane 2), there was a dramatic increase in p65 binding to the *cbs* promoter region for p65 binding site 1 (Fig. 9*A*, lane 5, *B*; $n = 3$ samples for each group, each sample having 2 rats, $^{**}p < 0.01$ compared with CON, 2-sample *t* test) and p65 binding site 2 (Fig. 9*C*, lane 5, *D*; $n = 3$ samples for each group, each sample having 2 rats, $^{*}p < 0.05$ ompared with CON, 2-sample *t* test) in STZ-treated rats compared with age- and sex-matched CON rats. These data indicated that the interaction between the p65 and *cbs* promoter regions was increased. We next investigated whether the enhanced interaction had an effect on *cbs* gene expression. Expression of p65 at protein levels was determined by Western blotting. STZ injection significantly increased the expression of p65 in T7–T10 DRGs when compared with age- and sex-matched CON rats (Fig. 9*E*; CON, $n = 5$, STZ, $n = 4$, $^{*}p < 0.05$ compared with CON, 2-sample *t* test). However, STZ injection did not significantly alter p65expression in T7–T10 DRGs in N-DM rats compared with age- and sex-matched CON rats (Fig. 9*F*; CON, $n = 4$, N-DM, $n = 4$, $p > 0.05$ compared with CON, 2-sample *t* test). We then determined whether upregulation of CBS expression was mediated by p65. Pyrrolidine dithiocarbamate (PDTC), an NF-κB inhibitor, was injected intraperitoneally at different doses once a day for seven consecutive days in STZ rats. PDTC markedly suppressed CBS expression at mRNA levels in STZ-treated rats (Fig. 9*G*; $n = 4$ for NS group; $n = 3$ for the rest each group, $^{**}p < 0.01$ compared with NS group; Tukey *post hoc* test after one-way ANOVA). PDTC injection at 50 mg/kg also significantly suppressed CBS expression at the protein level in STZ-treated rats (Fig. 9*H*; $n = 4$ for NS; $n = 5$ for PDTC, $^{*}p < 0.05$ compared with NS group, 2-sample *t* test).

## Discussion

In the present study, we attempted to elucidate a novel role for CBS-$H_2S$ signaling in gastric hypersensitivity and to show an epigenetic regulation of *cbs* gene expression in female rats made diabetic by STZ injection. We provide direct evidence that CBS-$H_2S$ signaling contributes to the development of gastric hypersensitivity in diabetic rats. In STZ-induced diabetes, a significant increase in behavioral responses to GD occurred 2 weeks after injection of STZ. The enhanced behavioral responses were maintained for at least another 4 weeks within our observation time period. This suggests the development of gastric hypersensitivity, making it a good model to mimic some of major characteristics in patients with diabetic gastroparesis. Further studies showed that STZ injection increased the expression of CBS in stomach DRGs and that blockade of CBS activity by AOAA significantly mitigated pain behavior in a dose-dependent fashion. These data suggest that the CBS-$H_2S$ signaling pathway plays a critical role in gastric hypersensitivity. Systemic administration of AOAA reduced behavioral responses in diabetic rats, but not in age- and sex-matched healthy CON rats, suggesting that this was not a nonspecific analgesic effect. This also suggests that the role of the CBS-$H_2S$ pathway in signaling GD may not be as important in healthy subjects as it is in those with sensitized pathophysiological conditions.

The pathophysiology of the gastrointestinal complications of diabetes is complex and multifactorial (Frøkjaer et al., 2007; Grabauskas et al., 2011). Several human studies indicate that neuropathy of enteric and autonomic nerves occurs in DM. Because changes in enteric neurons are likely to play a role in alterations in motility and secretory functions of the gastrointestinal tract (Chandrasekharan and Srinivasan, 2007), we focused our study on roles of primary sensory neurons. Recent studies implicated increased CBS-$H_2S$ signaling in the pathogenesis of a variety of neurodegenerative and inflammatory disorders (Yang et al., 2007; Schemann and Grundy, 2009). Here, we found that gastric projection neurons were hyperactive 4 weeks after STZ injection. This conclusion was evidenced by our observation of a significant depolarization in the RP, a lowered current stimulation threshold, a hyperpolarization in the AP threshold, and enhanced firing frequencies in response to a standardized stimulation and to a ramp stimulation in STZ rats compared with age- and sex-matched CON rats. Conversely, inhibition of CBS by AOAA significantly attenuated the AUC of EMGs and the neuronal excitability of gastric projection DRG neurons. These data indicate that hyperexcitability may be a hallmark for diabetic gastric hypersensitivity and that the CBS-$H_2S$ signaling pathway may therefore be of importance in the clinical setting.

The most significant finding in this study was that the molecular pathways involved in the regulation of *cbs* expression occur largely at the transcriptional level. We show that the *cbs* gene is an effective facilitator of STZ-stimulated gastric hypersensitivity, because a CBS inhibitor significantly attenuated behavioral responses to GD and suppressed neuronal hyperexcitability. The mechanism by which STZ increases expression of the *cbs* gene appears to involve the NF-κB signaling pathway, because upregulation of *cbs* expression was markedly reduced by the NF-κB inhibitor PDTC. This finding is consistent with our previous results showing that PDTC reduced CBS expression in lumbar DRGs in STZ-induced diabetic rats (Shi et al., 2013). However, how NF-κB regulates CBS expression remains unknown. In this study, we showed that p65 subunit DNA-binding ability in the *cbs* gene promoter was greatly potentiated in stomach DRGs from diabetic rats. This enhanced binding ability was most likely due to a significant DNA demethylation of the *cbs* promoter. Emerging evidence shows that DNA methylation suppresses gene expression, thus leading to gene silencing, whereas DNA demethylation facilitates gene upregulation. We showed here that promoter DNA of *cbs* gene was highly demethylated after STZ injection, which caused the upregulation of CBS expression at both the mRNA and protein levels in diabetic rats. To date, the mechanism of DNA demethylation remains largely unknown. It is well established that four members of DNMTs regulate DNA methylation in mammals: DNMT1 has high affinity for hemimethylated DNA and is believed to maintain the constitutive methylation status of DNA; DNMT2 does not have a DNA-binding domain and its role in methylation is unknown; and DNMT3a and DNMT3b are two major enzymes responsible for *de novo* methylation both in oncogenesis and in the responses to stressors in mammals. In this study, we observed demethylation of DNA in the *cbs* gene promoter (Fig. 6) and a decrease in DNMT3a and DNMT3b expression (Fig. 7*A*,*B*) in diabetic rats. Conversely, the expression of demethylation enzymes such as TDG, MBD2, and MBD4 was not significantly affected by the STZ treatment (Figs. 7*C*–*E*). These observations are consistent with the hypothesis that downregulation of DNMTs is a primary driving force for *cbs* gene demethylation after STZ-induced diabetes, a passive rather than an active gene demethylation mechanism. This is different from our previously published results showing that an active mechanism is involved in inflammatory pain (Qi et al., 2013). Although the detailed mechanisms for this difference is unknown, it is possible that mechanisms of diabetic gastric hypersensitivity may be different from those of inflammatory somatic pain, further supporting that epigenetic regulation may be disease and/or organ specific. These findings suggest for the first time that an epigenetic regulation might be involved in the development of gastric hypersensitivity by enhancing NF-κB-mediated *cbs* gene expression. Together with previous results (Zhang et al., 2011; Qi et al., 2013), the results of the present study provide further evidence for the involvement of epigenetic mechanisms in chronic pain.

In conclusion, we demonstrate for the first time to our knowledge that diabetic gastric hypersensitivity is mediated by enhanced upregulation of CBS expression resulting from abnormal binding of upregulation of NF-κB with the demethylated *cbs* gene in stomach DRG neurons. Our *in vitro* experiments also provide evidence that $H_2S$ contributes to neuronal excitability of DRG innervating the stomach, thus leading to gastric hypersensitivity. Conventional treatment of diabetic gastric hypersensitivity, including the use of morphine, has not been effective because of drug side effects (Kashyap and Farrugia, 2010; Lee and Kuo, 2010). Our results suggest that modification of the NF-κB–CBS pathway may prove to be a useful alternative strategy for the treatment of diabetic-related gastrointestinal disorders. Further advances in our understanding of the epigenetic regulations will have important implications for the treatment of diabetes-related gastrointestinal disorders.

## References

Anitha M, Gondha C, Sutliff R, Parsadanian A, Mwangi S, Sitaraman SV, Srinivasan S (2006) GDNF rescues hyperglycemia-induced diabetic enteric neuropathy through activation of the PI3K/Akt pathway. J Clin Invest 116:344–356. CrossRef Medline

Beyak MJ, Bulmer DC, Sellers D, Grundy D (2009) Impairment of rectal afferent mechanosensitivity in experimental diabetes in the rat. Neurogastroenterol Motil 21:678–681. CrossRef Medline

Bytzer P, Talley NJ, Leemon M, Young LJ, Jones MP, Horowitz M (2001) Prevalence of gastrointestinal symptoms associated with diabetes melli-

tus: a population-based survey of 15,000 adults. Arch Intern Med 161: 1989–1996. CrossRef Medline

Chandrasekharan B, Srinivasan S (2007) Diabetes and the enteric nervous system. Neurogastroenterol Motil 19:951–960. CrossRef Medline

Frøkjaer JB, Andersen SD, Ejskaer N, Funch-Jensen P, Arendt-Nielsen L, Gregersen H, Drewes AM (2007) Gut sensations in diabetic autonomic neuropathy. Pain 131:320–329. CrossRef Medline

Frøkjaer JB, Søfteland E, Graversen C, Dimcevski G, Egsgaard LL, Arendt-Nielsen L, Drewes AM (2009) Central processing of gut pain in diabetic patients with gastrointestinal symptoms. Diabetes Care 32:1274–1277. CrossRef Medline

Frøkjaer JB, Egsgaard LL, Graversen C, Søfteland E, Dimcevski G, Blauenfeldt RA, Drewes AM (2011) Gastrointestinal symptoms in type-1 diabetes: is it all about brain plasticity? Eur J Pain 15:249–257. CrossRef Medline

Frommer M, McDonald LE, Millar DS, Collis CM, Watt F, Grigg GW, Molloy PL, Paul CL (1992) A genomic sequencing protocol that yields a positive display of 5-methylcytosine residues in individual DNA strands. Proc Natl Acad Sci U S A 89:1827–1831. CrossRef Medline

Grabauskas G, Heldsinger A, Wu X, Xu D, Zhou S, Owyang C (2011) Diabetic visceral hypersensitivity is associated with activation of mitogen-activated kinase in rat dorsal root ganglia. Diabetes 60:1743–1751. CrossRef Medline

He CL, Soffer EE, Ferris CD, Walsh RM, Szurszewski JH, Farrugia G (2001) Loss of interstitial cells of cajal and inhibitory innervation in insulin-dependent diabetes. Gastroenterology 121:427–434. CrossRef Medline

Herman JG, Graff JR, Myöhänen S, Nelkin BD, Baylin SB (1996) Methylation-specific PCR: a novel PCR assay for methylation status of CpG islands. Proc Natl Acad Sci U S A 93:9821–9826. CrossRef Medline

Hoogerwerf WA, Pasricha PJ, Kalloo AN, Schuster MM (1999) Pain: the overlooked symptom in gastroparesis. Am J Gastroenterol 94:1029–1033. CrossRef Medline

Hunt SP, Mantyh PW (2001) The molecular dynamics of pain control. Nat Rev Neurosci 2:83–91. CrossRef Medline

Kashyap P, Farrugia G (2010) Diabetic gastroparesis: what we have learned and had to unlearn in the past 5 years. Gut 59:1716–1726. CrossRef Medline

Kordi-Tamandani DM, Moazeni-Roodi AK, Rigi-Ladiz MA, Hashemi M, Birjandian E, Torkamanzehi A (2010) Promoter hypermethylation and expression profile of MGMT and CDH1 genes in oral cavity cancer. Arch Oral Biol 55:809–814. CrossRef Medline

Lee A, Kuo B (2010) Metoclopramide in the treatment of diabetic gastroparesis. Expert Rev Endocrinol Metab 5:653–662. CrossRef Medline

Li L, Xie R, Hu S, Wang Y, Yu T, Xiao Y, Jiang X, Gu J, Hu CY, Xu GY (2012) Upregulation of cystathionine beta-synthetase expression by nuclear factor-kappa B activation contributes to visceral hypersensitivity in adult rats with neonatal maternal deprivation. Mol Pain 8:89. CrossRef Medline

Liao D, Zhao J, Gregersen H (2006) Three-dimensional geometry analysis of the stomach in type II diabetic GK rats. Diabetes Res Clin Pract 71:1–13. CrossRef Medline

Liu LS, Shenoy M, Pasricha PJ (2011) The analgesic effects of the GABAB receptor agonist, baclofen, in a rodent model of functional dyspepsia. Neurogastroenterol Motil 23:356–361, e160–e351. CrossRef Medline

Owyang C (2011) Phenotypic switching in diabetic gastroparesis: mechanism directs therapy. Gastroenterology 141:1134–1137. CrossRef Medline

Qi F, Zhou Y, Xiao Y, Tao J, Gu J, Jiang X, Xu GY (2013) Promoter demethylation of cystathionine-beta-synthetase gene contributes to inflammatory pain in rats. Pain 154:34–45. CrossRef Medline

Samsom M, Akkermans LM, Jebbink RJ, van Isselt H, vanBerge-Henegouwen GP, Smout AJ (1997) Gastrointestinal motor mechanisms in hyperglycaemia induced delayed gastric emptying in type I diabetes mellitus. Gut 40:641–646. Medline

Schemann M, Grundy D (2009) Role of hydrogen sulfide in visceral nociception. Gut 58:744–747. CrossRef Medline

Shi L, Zhang H, Xiao Y, Hu J, Xu GY (2013) Electroacupuncture suppresses mechanical allodynia and nuclear factor kappa B signaling in streptozotocin-induced diabetic rats. CNS Neurosci Ther 19:83–90. CrossRef Medline

Srinivasan S, Wiley JW (2000) New insights into neural injury, repair, and adaptation in visceral afferents and the enteric nervous system. Curr Opin Gastroenterol 16:78–82. CrossRef Medline

Turek-Plewa J, Jagodziński PP (2005) The role of mammalian DNA methyltransferases in the regulation of gene expression. Cell Mol Biol Lett 10:631–647. Medline

Vinik AI, Maser RE, Mitchell BD, Freeman R (2003) Diabetic autonomic neuropathy. Diabetes Care 26:1553–1579. CrossRef Medline

Wang C, Ning LP, Wang YH, Zhang Y, Ding XL, Ge HY, Arendt-Nielsen L, Yue SW (2011) Nuclear factor-kappa B mediates TRPV4-NO pathway involved in thermal hyperalgesia following chronic compression of the dorsal root ganglion in rats. Behav Brain Res 221:19–24. CrossRef Medline

Wang Y, Qu R, Hu S, Xiao Y, Jiang X, Xu GY (2012) Upregulation of Cystathionine beta-Synthetase Expression Contributes to Visceral Hyperalgesia Induced by Heterotypic Intermittent Stress in Rats. PLoS One 7:e53165. CrossRef Medline

Watkins CC, Sawa A, Jaffrey S, Blackshaw S, Barrow RK, Snyder SH, Ferris CD (2000) Insulin restores neuronal nitric oxide synthase expression and function that is lost in diabetic gastropathy. J Clin Invest 106:373–384. CrossRef Medline

Xu GY, Huang LY (2002) Peripheral inflammation sensitizes P2X receptor-mediated responses in rat dorsal root ganglion neurons. J Neurosci 22:93–102. Medline

Xu GY, Shenoy M, Winston JH, Mittal S, Pasricha PJ (2008) P2X receptor-mediated visceral hyperalgesia in a rat model of chronic visceral hypersensitivity. Gut 57:1230–1237. CrossRef Medline

Xu GY, Winston JH, Shenoy M, Zhou S, Chen JD, Pasricha PJ (2009) The endogenous hydrogen sulfide producing enzyme cystathionine-beta synthase contributes to visceral hypersensitivity in a rat model of irritable bowel syndrome. Mol Pain 5:44. CrossRef Medline

Xu GY, Li G, Liu N, Huang LY (2011) Mechanisms underlying purinergic P2X3 receptor-mediated mechanical allodynia induced in diabetic rats. Mol Pain 7:60. CrossRef Medline

Yang G, Yang W, Wu L, Wang R (2007) H2S, endoplasmic reticulum stress, and apoptosis of insulin-secreting beta cells. J Biol Chem 282: 16567–16576. CrossRef Medline

Zhang Z, Cai YQ, Zou F, Bie B, Pan ZZ (2011) Epigenetic suppression of GAD65 expression mediates persistent pain. Nat Med 17:1448–1455. CrossRef Medline